The chemoattractant chemerin suppresses melanoma by recruiting natural killer cell antitumor defenses

Russell K. Pachynski,[1,2,5] Brian A. Zabel,[6] Holbrook E. Kohrt,[2] Nicole M. Tejeda,[1,5] Justin Monnier,[1,5,6] Christina D. Swanson,[3,6] Alison K. Holzer,[1,5] Andrew J. Gentles,[4] Gizette V. Sperinde,[1,5] Abdolhossein Edalati,[1,5] Husein A. Hadeiba,[1,5,6] Ash A. Alizadeh,[2] and Eugene C. Butcher[1,5]

[1]Laboratory of Immunology and Vascular Biology, Department of Pathology; [2]Division of Oncology and [3]Division of Immunology and Rheumatology, Department of Medicine; and [4]Department of Radiology; Stanford University School of Medicine, Stanford, CA 94305

[5]Center for Molecular Biology and Medicine and [6]Palo Alto Institute for Research and Education, Veterans Affairs Palo Alto Health Care System, Palo Alto, CA 94304

Infiltration of specialized immune cells regulates the growth and survival of neoplasia. Here, in a survey of public whole genome expression datasets we found that the gene for chemerin, a widely expressed endogenous chemoattractant protein, is down-regulated in melanoma as well as other human tumors. Moreover, high chemerin messenger RNA expression in tumors correlated with improved outcome in human melanoma. In experiments using the B16 transplantable mouse melanoma, tumor-expressed chemerin inhibited in vivo tumor growth without altering in vitro proliferation. Growth inhibition was associated with an altered profile of tumor-infiltrating cells with an increase in natural killer (NK) cells and a relative reduction in myeloid-derived suppressor cells and putative immune inhibitory plasmacytoid dendritic cells. Tumor inhibition required host expression of CMKLR1 (chemokine-like receptor 1), the chemoattractant receptor for chemerin, and was abrogated by NK cell depletion. Intratumoral injection of chemerin also inhibited tumor growth, suggesting the potential for therapeutic application. These results show that chemerin, whether expressed by tumor cells or within the tumor environment, can recruit host immune defenses that inhibit tumorigenesis and suggest that down-regulation of chemerin may be an important mechanism of tumor immune evasion.

CORRESPONDENCE
Russell K. Pachynski:
rkpachynski@stanford.edu

Abbreviations used: MDSC, myeloid-derived suppressor cell; pDC, plasmacytoid DC; TIL, tumor-infiltrating leukocyte.

To survive and flourish, malignant cells must elude or subvert antitumor immune responses. Malignant cells can down-regulate NK cell target molecules and major histocompatibility antigens recognized by cytotoxic T cells or up-regulate inhibitory receptors such as the anti–phagocytic signal CD47 (Majeti et al., 2009). Tumors also take advantage of mechanisms of natural self-tolerance, recruiting tolerogenic DCs and inducing immunosuppressive regulatory T cells and myeloid-derived suppressor cells (MDSCs) that inhibit cytotoxic antitumor responses (Maldonado and von Andrian, 2010; Nagaraj and Gabrilovich, 2010). Infiltrating leukocytes can also contribute to tumor survival by producing growth factors and stimulating angiogenesis. Conversely, antitumor effector cells can arrest the development or expansion of malignancies: NK cells are important mediators of innate antitumor immunity, and immunostimulatory DCs and cytotoxic T cells participate in tumor suppression as well (Zitvogel et al., 2006). Ultimately, the balance between pro- and antitumor leukocytes determines the behavior and fate of transformed cells. However, the physiological mechanisms responsible for effector cell recruitment for immune surveillance remain poorly understood.

The Rockefeller University Press $30.00
J. Exp. Med. 2012 Vol. 209 No. 8 1427-1435
www.jem.org/cgi/doi/10.1084/jem.20112124

The Journal of Experimental Medicine

In this study, we present evidence that chemerin, a recently described chemoattractant for NK cells, macrophages, and DC subsets (Wittamer et al., 2003; Zabel et al., 2005; Parolini et al., 2007), is a physiologically important mediator of antitumor immunity and immune surveillance. We show that the gene for chemerin (*RARRES2* [*retinoic acid receptor responder* (tazarotene induced) *2*]) is down-regulated in melanoma and in many other human solid tissue neoplasms and that higher expression correlates with improved clinical outcomes in melanoma. Moreover, in a mouse model of melanoma, expression or intratumoral administration of chemerin enhanced the infiltration of NK cells into tumors, altered the ratio of NK cells to myeloid suppressor cells, and inhibited tumor growth in an NK cell–dependent manner. We conclude that chemerin recruits antitumor immune effector cells and that it may act as an endogenous tumor

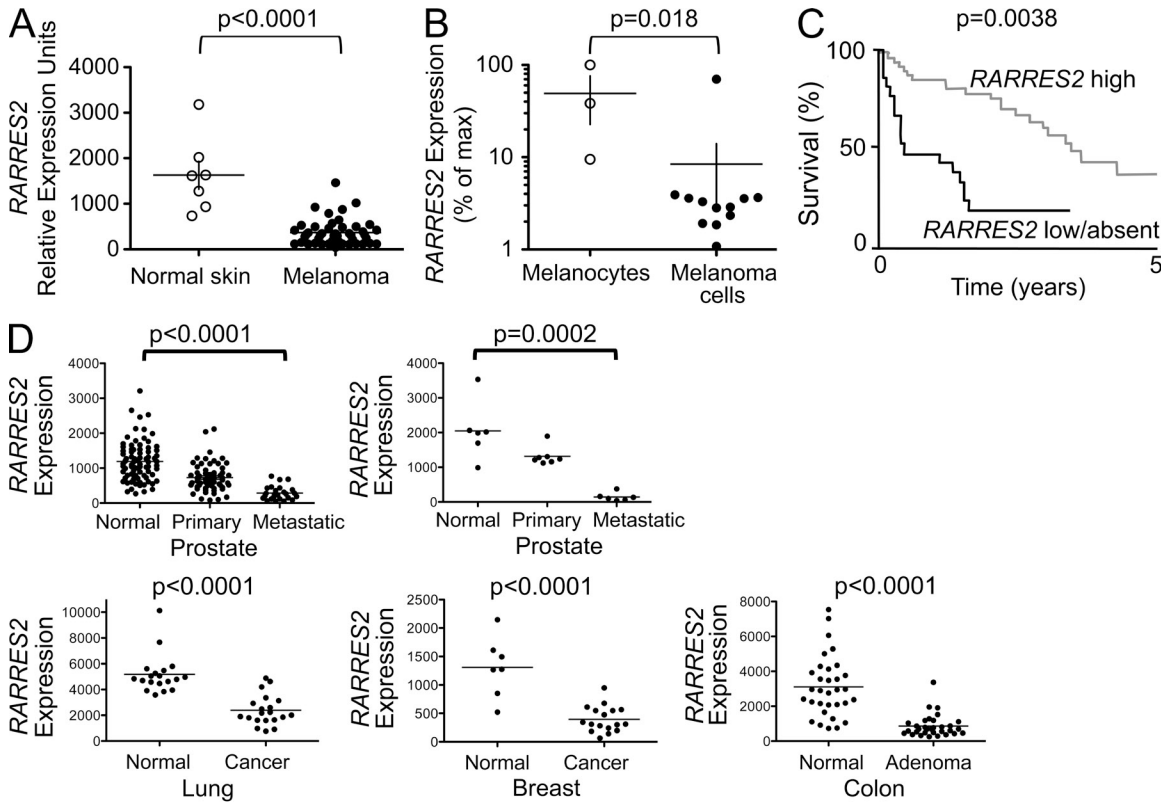

E

Disease (dataset)	Data Source	Patients (n)	Therapy	HR	z-score	p-value
Melanoma (1)	NCBI GEO: GSE8401	39	surgical resection or chemo (various)	0.7	-3.181	<0.002
Melanoma (2)	EBI Array Express: E-TABM-1	81	surgical resection	0.023	-2.798	0.005

Figure 1. Down-regulation of *RARRES2* in human tumors. (A) *RARRES2* expression in melanoma and in normal skin. Public microarray data from the GEO database (accession no. GDS1375) showing the relative expression (calculated signal intensities) of *RARRES2* (chemerin). Individual tissue samples are represented as dots. Two-tailed Student's *t* test was used to determine statistical significance. (B) Publically available datasets from the GEO database that had direct comparisons of *RARRES2* expression in both melanocyte and melanoma primary cultures or cell lines were identified ($n = 2$; GDS1965 and GDS3012). Data were normalized to GAPDH and pooled and shown as percentage of maximal *RARRES2* expression. Significance was determined using the Mann-Whitney test. (A and B) Horizontal bars represent the mean, and vertical bars represent SEM. (C) Kaplan-Meier plot of overall survival for both high and low/absent *RARRES2* expression cohorts relative to an idealized threshold, with associated log-rank p-values shown after correction for multiple hypothesis testing using 1,000-fold cross-validation. (D) *RARRES2* expression was evaluated in GDS datasets in the GEO database from studies comparing precancerous, primary, or metastatic solid tumors with appropriate normal tissue counterparts. Tumor tissues of prostate cancer (two), colon adenoma, and breast and lung adenocarcinoma (GDS2545, GDS1375, GDS2947, GDS1650, GDS2250, and GDS1439) were examined. Two-tailed Student's *t* test was used to determine statistical significance. Individual tissue samples are represented as dots, and bars represent mean. For significant differences, the p-value is noted. (E) Summary of statistical analyses is presented from two clinical datasets (Winnepenninckx et al., 2006; Xu et al., 2008). Statistics are presented for *RARRES2* expression when considered as a continuous variable with log-likelihood p-values within a univariate Cox regression model. Therapy represents all possible therapies administered within each cohort. HR, hazard ratio.

suppressor whose down-regulation in melanoma and potentially other tumors could contribute to immune evasion and tumor growth.

RESULTS AND DISCUSSION

We assessed expression of the gene encoding the chemoattractant chemerin (*RARRES2*) in well-annotated NCBI GEO datasets (Edgar et al., 2002) comparing patient tumors with their normal tissue counterparts. *RARRES2* was significantly down-regulated in melanomas (Fig. 1 A) and in many human solid tumors, including prostate, breast and lung adenocarcinomas, and colon adenomas (Fig. 1 D). Consistent with these analyses of curated public datasets, down-regulation of *RARRES2* has been reported in studies of several specific tumor types in human, including colon, adrenocortical, prostate, and skin carcinomas (Stamey et al., 2001; Fernandez-Ranvier et al., 2008; Segditsas et al., 2008; Zheng et al., 2008). Such down-regulation may involve cell-autonomous *RARRES2* suppression during malignant transformation: *RARRES2* expression was reduced in melanoma cells compared with primary melanocyte cultures (Fig. 1 B). Moreover, Zheng et al. (2008) reported that epithelial expression of *RARRES2* (assessed by in situ hybridization) and chemerin protein (by immunohistochemistry) is lost during development of squamous carcinoma in the skin. However, down-regulation in tumor samples could also reflect changes in representation or gene expression by chemerin-expressing nonmalignant stromal cell populations.

Importantly, retention of high *RARRES2* expression correlated with better outcomes in two independent clinical experiments of melanoma (Fig. 1, C and E). The *RARRES2* gene product chemerin is a recently described chemoattractant for NK cells and subsets of DCs (Wittamer et al., 2003; Zabel et al., 2005; Parolini et al., 2007), innate immune cells implicated in antitumor responses. An inactive prochemerin circulates in blood and can be activated by diverse proteases associated with inflammation and tissue injury (Zabel et al., 2006), but local chemerin expression in tissues is thought to regulate the recruitment of cells expressing the functional chemerin receptor CMKLR1 (chemokine-like receptor 1; Parolini et al., 2007; Skrzeczyńska-Moncznik et al., 2009). We also found a significant correlation between *RARRES2* expression and the NK-restricted gene (*KLRD1*; Su et al., 2004; $r = 0.25$, $P < 0.0001$) and with a panel of 16 NK-specific genes as defined within the same dataset and most correlated with *KLRD1* (i.e., NK signature comprising: *KIR3DL1*, *PTGDR*, *CD160*, *KLRF1*, *LOC727787*, *KLRC3*, *SIGLECP3*, *KLRD1*, *TRDA*, *XCL1*, *XCL2*, *SH2D1B*, *KIR3DS1*, *LAIR2*, *KIR2DL4*, and *KIR2DL3*; $r = 0.12$, $P < 0.0001$) in datasets of human melanoma and multiple tumor types (not depicted), suggesting a link between chemerin and tumor-infiltrating NK cells in humans. Given the frequent down-regulation of *RARRES2* in malignant tumors and its inverse correlation with outcome in melanoma, we hypothesized that local chemerin expression by malignant or surrounding normal tissue cells might be deleterious to melanoma cell survival or tumor progression.

To test this hypothesis, we first compared the phenotype and the growth characteristics of chemerin-expressing versus control lines of a well-characterized transplantable mouse melanoma, B16F0. *RARRES2* transfectants but not host B16 or control vector transfectants secreted chemerin (Fig. 2 A).

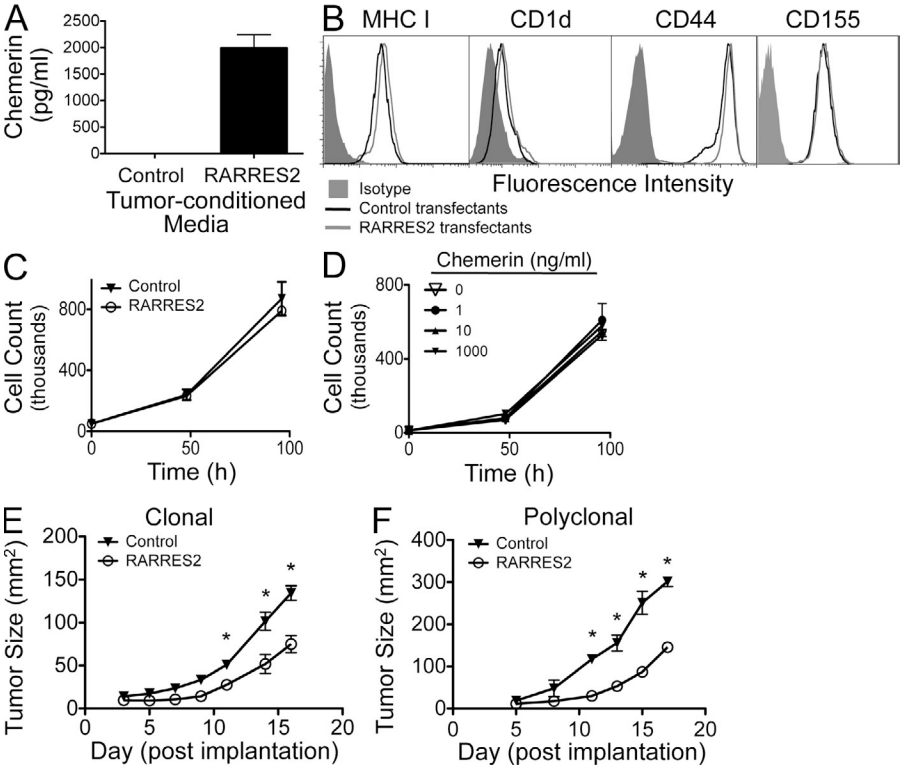

Figure 2. Overexpression of chemerin suppresses tumor growth. (A) Measurement by ELISA of secreted chemerin in conditioned media from control or *RARRES2*-transfected B16 melanoma cells. (B) FACS analysis of the surface phenotype of transfected B16 lines. (C and D) In vitro proliferation of *RARRES2*-transfected and untransfected, wild-type B16 melanoma cells (C) or after culturing with recombinant chemerin (D). (A, C, and D) Error bars represent SEM. (E and F) Clonal (E) and polyclonal (F) chemerin-expressing or control vector–transfected B16 cells were implanted subcutaneously into C57BL/6 mice, and growth was measured over time. Graphs are from a representative experiment of more than four performed with two independently derived chemerin-expressing clones (E) or independently generated polyclonal transfectant pools (F). Tumor size is represented as mean ± SEM, with cohorts of more than four mice per group. *, $P < 0.05$ comparing control versus chemerin-expressing tumors by two-tailed Student's *t* test.

The bioactivity of secreted chemerin was confirmed by its ability to recruit a CMKLR1$^+$ lymphoid cell line in in vitro chemotaxis assays (not depicted). The *RARRES2* transfectants retained surface expression of MHC class I (involved in CD8$^+$ T cell recognition), CD1d (important for NK cell recognition), CD44 (implicated in tumor invasion and metastasis), and CD155 (a key ligand in NK cell suppression of melanoma progression) at levels similar to control transfectants (Fig. 2 B); as expected, other NK cell receptors (CD48, CD226, CD335, and NKG2D) were not expressed (not depicted). Importantly, B16 cells lack known receptors for chemerin (not depicted), and neither chemerin expression by transfectants (Fig. 2 C) nor exogenously added chemerin altered their in vitro proliferation or expansion (Fig. 2 D). However, when implanted subcutaneously into mice, chemerin-expressing melanomas grew more slowly than control transfectants (Fig. 2 E). Two independently derived chemerin-expressing B16 clones displayed similarly impaired growth (not depicted), suggesting that the effect is chemerin dependent and not a consequence of clonal variation. Polyclonal *RARRES2*-transfected B16 populations also grew poorly compared with bulk vector control–transfected cells (Fig. 2 F), further ruling out clonal effects. Together these findings show that autochthonous chemerin impairs tumor growth in vivo and suggest that this growth inhibition reflects an alteration in the host environment rather than a direct effect on the malignant cells themselves.

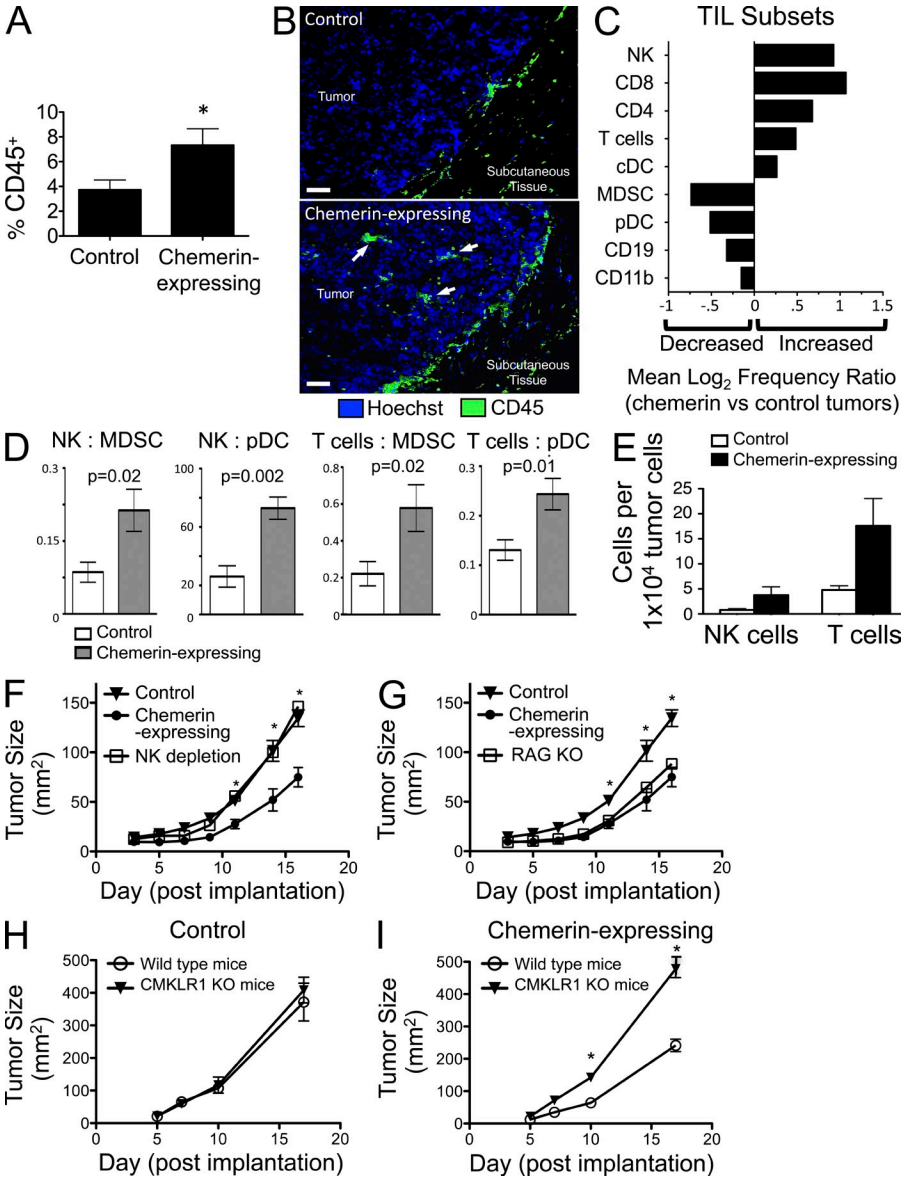

Figure 3. Overexpression of chemerin increases the number and alters the make up of TILs. (A) CD45$^+$ leukocyte infiltration (percentage of viable cells) from chemerin-expressing versus control tumors excised on day 17 and analyzed by flow cytometry. *, $P < 0.05$ by two-tailed Student's *t* test. (B) Immunofluorescence images illustrate CD45$^+$ cell infiltrates (arrows) in chemerin-expressing melanomas excised at day 9. Bars, 25 µm. (C) Log_2 ratio of TIL subset frequency in chemerin-expressing versus control tumors as calculated from FACS analyses of pDCs (Lin$^-$CD11c^{int}B220$^+$PDCA1$^+$), conventional DCs (cDCs; Lin$^-$CD11c^{hi}B220$^-$), CD4 (CD3$^+$CD4$^+$) T cells, CD8 (CD3$^+$CD8$^+$) T cells, total T cells (CD3$^+$CD4$^+$CD8$^+$), NK cells (CD3$^-$NK1.1$^+$), CD11b (Lin$^-$CD11b$^+$) monocyte/macrophages, MDSCs (Lin$^-$CD11b$^+$GR1$^+$), and CD19$^+$ B cells (CD3$^-$CD19$^+$). (D) Ratio of NK or total T cells to MDSCs or pDCs in tumors. (E) Absolute numbers of NK and T cells per 10,000 total tumor cells analyzed by FACS from control or chemerin-expressing tumors. Results are from a representative experiment. (A, D, and E) Graphs show mean ± SEM with four or more mice per group. (F) Control ($n = 5$) or chemerin-expressing B16 ($n = 5$) was orthotopically implanted into C57BL/6 wild-type mice. Anti–Asialo GM1 depleting antibody was used to deplete NK cells in mice bearing chemerin-expressing tumors (NK depletion; $n = 8$). *, $P < 0.05$ comparing tumor size (mean ± SEM) in control or chemerin-expressing versus NK depletion by two-tailed Student's *t* test. Data are representative of three experiments. (G) Chemerin-expressing B16 cells were orthotopically implanted in C57BL/6 wild-type and RAG1 KO mice (RAG KO; $n = 9$) and compared with control B16 cells implanted in WT mice. *, $P < 0.05$ comparing tumor size (mean ± SEM) in chemerin-expressing or RAG KO versus control by two-tailed Student's *t* test. Data are representative of two experiments. (H and I) Control (H) or chemerin-expressing (I) B16 cells were implanted into WT or CMKLR1 KO mice ($n = 5$/group), and tumor growth was assessed. *, $P < 0.05$ comparing tumor size (mean ± SEM) in WT versus CMKLR1 KO with implanted chemerin-expressing tumors by two-tailed Student's *t* test.

Chemerin expression enhanced the infiltration of leukocytes and altered the relative representation of effector and antigen-presenting cell subsets. There was a significant increase in CD45$^+$ cells in dissociated cell suspensions of chemerin-expressing tumors compared with controls (Fig. 3 A). Increased infiltration of CD45$^+$ cells in the chemerin-expressing tumors was also evident by immunofluorescence microscopy (Fig. 3 B). On average, the frequency of conventional DCs (Lin$^-$B220$^-$CD11c$^+$), T cells, and NK cells was increased in chemerin-expressing tumors, with a concomitant decrease in the percentage of MDSCs (Lin$^-$CD11b$^+$GR1$^+$) and plasmacytoid DCs (pDCs; Lin$^-$B220$^+$CD11c^{int}PDCA1$^+$), which are considered tolerogenic (Fig. 3 C; Hadeiba et al., 2008; Ostrand-Rosenberg, 2010); importantly, the absolute numbers of NK and T cells per tumor cells were increased, and the ratios of NK cells and of total T cells to MDSCs or to pDCs among tumor-infiltrating leukocytes (TILs) were significantly increased (Fig. 3, D and E). Such ratios of effector to suppressor cell populations can have a significant impact on tumor growth (Sato et al., 2005; Curran et al., 2010) and may be important in the overall pro/antitumor balance of the tumor microenvironment (Schreiber et al., 2011).

Given the increase in tumor-infiltrating NK cells and T cells, we next asked whether these lymphocyte subsets played a role in chemerin-mediated suppression of melanoma growth. NK cell depletion completely abrogated the anti-melanoma effect, resulting in rapid growth of the chemerin-expressing tumors, similar to that of control tumors (Fig. 3 F). In contrast, the absence of T and B cells in RAG1-deficient hosts had no effect on chemerin inhibition of the melanoma (Fig. 3 G). Thus, the inhibitory effect of chemerin on B16 melanoma growth is mediated by host NK cells, whereas T and B cells are not required. Chemerin did not affect the function of resting or IL2-activated NK cells in standard assays of cytotoxic function, nor did chemerin induce NK cytokine release (not depicted). NK cell activation was also not affected by chemerin (Fig. 4 A), suggesting that its primary effect on NK cells may be to mediate their recruitment to the tumor environment. Indeed, CMKLR1$^+$ normal leukocytes, including NK cells and DC subsets, are known to migrate toward chemerin in chemotaxis assays (Wittamer et al., 2003; Zabel et al., 2005; Parolini et al., 2007; Skrzeczyńska-Moncznik et al., 2009). Importantly, the chemerin–CMKLR1 pathway has also been implicated in the recruitment of NK cells into inflamed pathological peripheral tissues (Parolini et al., 2007; Skrzeczyńska-Moncznik et al., 2009). Consistent with this, we found that both peripheral blood and tumor-infiltrating NK cells expressed CMKLR1 (not depicted).

Chemerin attracts cells expressing the receptor CMKLR1. To determine whether chemerin-mediated tumor suppression required host expression of this chemerin receptor, we compared tumor growth in wild-type versus CMKRL1-deficient mice. There was no difference in growth of control B16 tumors in wild-type or CMKLR1$^{-/-}$ mice (Fig. 3 H). However, chemerin-expressing B16 tumors grew significantly more rapidly, indistinguishably from control tumors, in CMKLR1$^{-/-}$ hosts (Fig. 3 I). These results were confirmed using a second, independently derived chemerin-expressing B16 clone (not depicted). We conclude that in this model, CMKLR1 expression by host cells is required for chemerin to effectively suppress tumor growth. Overall, these experiments show that host NK cells and CMKLR1 are necessary for the suppressive effect of chemerin on melanoma growth in vivo in the mouse tumor model.

To determine whether chemerin in the local environment might be sufficient to inhibit the proliferation of malignant cells, we assessed the growth of wild-type B16 cells treated with local or intratumoral chemerin injections. In some experiments, chemerin was administered daily starting at the time of tumor cell implantation. In other experiments, chemerin was injected into established tumors starting ~5–7 d after cell inoculation, when the tumors

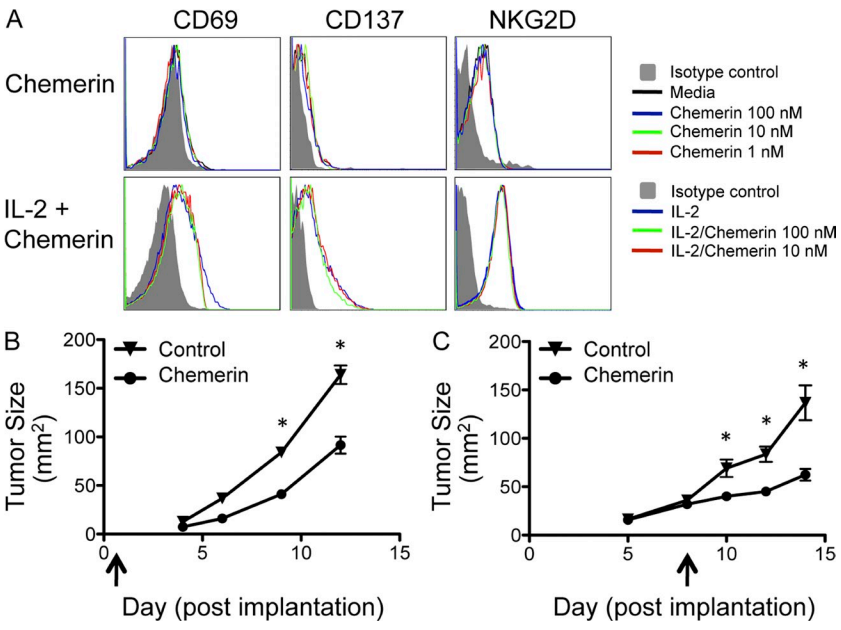

Figure 4. Effects of exogenous chemerin on NK cell activation and tumor growth. (A) Untouched murine NK cells were isolated using the MACS NK Isolation kit II (Miltenyi Biotec) and cultured with or without 25 ng/ml IL-2 and/or active murine chemerin using the indicated conditions for 24 h. NK cells were then evaluated by flow cytometry for the activation phenotype. (B and C) Daily intratumoral injections of control (PBS or murine serum albumin) or recombinant active chemerin (25–250 ng/dose) were initiated at the time of tumor cell implantation (B) or after palpable tumors had established (C), as indicated by the arrows. *, $P < 0.05$ comparing tumor size (mean ± SEM) in chemerin injection versus control by two-tailed Student's *t* test. Data are representative of three experiments (B) or more than five experiments (C), with cohorts of more than three mice per group.

were palpable. Administration of active chemerin either from the time of inoculation or after establishment of tumors significantly inhibited tumor growth (Fig. 4, B and C, respectively). The results suggest that local expression of chemerin by cells in the environment of a transformed cell, or within tumor stroma, could contribute to tumor control.

Chemerin differs in many respects from previously described "tumor-suppressive cytokines," many of which were initially defined based on their direct effects on tumor cells. Examples include the proinflammatory factors TNF and IL1-β and the immunoregulatory TGF-β. These cytokines may also marshal host responses and inhibit tumor growth in certain settings (Apte et al., 2006; Sethi et al., 2008; Bierie and Moses, 2010). In contrast to the down-regulation of chemerin, genes encoding these cytokines are not suppressed in melanomas (not depicted). Neoplastic cells thus must have mechanisms to escape the antitumor effects of these "suppressors," and in fact, as in the case of TGF-β, may sometimes use them to their advantage for the development and support of tumor growth (Apte et al., 2006; Sethi et al., 2008; Bierie and Moses, 2010). We cannot exclude the possibility that chemerin effects in cancer can also be tumor or context dependent. Chemoattractants with restricted tissue expression may also contribute to tumor resistance: indeed, CCL27 (chemokine ligand 27), a keratinocyte-restricted chemokine, is down-regulated like chemerin in human cutaneous squamous carcinoma (Pivarcsi et al., 2007). Antibody neutralization of CCL27 allowed enhanced growth of transplanted melanoma cells in mice associated with reduced T cell infiltration, although the importance of recruited leukocytes versus direct CCL27 effects on tumor cell proliferation and survival was not assessed in this study (Pivarcsi et al., 2007). Interestingly, *RARRES2* is transcriptionally up-regulated in skin by retinoic acid (Nagpal et al., 1997), and retinoid signaling is often suppressed in melanoma (Chakravarti et al., 2007). Thus, although other transcription factors (such as peroxisome proliferator–activated receptor γ) also likely regulate *RARRES2* expression (Muruganandan et al., 2011), it is possible that in melanoma, reduced retinoid receptor activation may contribute to *RARRES2* down-regulation. Conversely, chemerin induction could contribute to the therapeutic effects of retinoids, tazarotene in particular (Shistik et al., 2007), in melanoma (Klopper et al., 2009).

Together, our findings show that, whether expressed by malignant cells themselves or within the tumor environment, chemerin can recruit host defenses and inhibit melanoma growth. Together with the correlation of retained high *RARRES2* expression with improved clinical outcomes in melanoma, the results suggest that locally expressed chemerin may act as an endogenous tumor-suppressive chemoattractant. Treatment modalities that preserve or enhance local chemerin expression by transformed or tumor stromal cells, or targeted approaches that deliver chemerin to tumors, may effectively engage the body's endogenous mechanisms of tumor resistance and suppression.

MATERIALS AND METHODS

Microarray data analyses. For human clinical cases, *RARRES2* expression was evaluated in GDS datasets from studies comparing primary or metastatic solid tumors with appropriate normal tissue counterparts. Only studies that used the Affymetrix platforms and in which GAPDH GC-RMA signals were robust (>7,000 for U95 probe M33197_M_at or for U133 probe 213453_x_at) and which included ≥5 normal samples and ≥10 neoplastic samples were evaluated. Seven datasets met these criteria. *RARRES2* was significantly down-regulated in tumor tissues in studies of melanoma, prostate cancer (two), colon adenoma, and lung and breast adenocarcinoma (GEO DataSets accession nos. GDS1375 [Fig. 1 A], GDS2545 and GDS1439, GDS2947, GDS1650, and GDS2250 [Fig. 1 D], respectively). The gene was up-regulated in one dataset involving comparisons of clear cell carcinoma of the kidney with normal kidney (GDS2880). Significance of differences in *RARRES2* expression in sample groups was determined using the unpaired Student's *t* test.

Analysis of the prognostic value of *RARRES2* expression in human malignancies. *RARRES2* messenger RNA gene expression and clinical data were analyzed for two previously described patient cohorts with malignant melanoma (see Fig. 1 E for detailed dataset descriptions). Association between *RARRES2* expression and clinical outcome was assessed by examining continuous expression of *RARRES2* in relation to overall survival as measured by log-likelihood p-values within a univariate Cox regression model (Fig. 1 C); hazard ratios reflect risk of death per twofold change in *RARRES2* messenger RNA expression as measured within each cohort. Patients were separately analyzed for overall survival by Kaplan-Meier analysis and stratified into high and low *RARRES2* groups based on comparison of expression level relative to an idealized threshold within each cohort. Multiple hypothesis testing correction for optimal threshold selection was addressed using 1,000-fold cross-validation within each experiment; for corresponding the Kaplan Meier strata depicted as survival curves (Fig. 1 C), only these corrected log-rank p-values are reported. Affymetrix microarray data were processed starting with CEL files, with Entrez Gene probe set summarization using CustomCDF version 12 and normalization using MAS 5.0 linear scaling method.

Mice and cell lines. For all animal experiments, C57BL/6 or B6.129S7-*Rag1*^{tm1Mom}/J (RAG1 KO) mice were purchased from the Jackson Laboratory. CMKLR1 KO mice that were fully backcrossed onto the C57BL/6 background were obtained from Deltagen; these have been shown to be phenotypically similar to WT mice in a previous study (Ernst et al., 2012). Mice were maintained in our facilities at the Palo Alto Veterinary Medical Unit and used at ∼8–12 wk of age. All animal experiments were conducted in accordance with approved Stanford University and National Institutes of Health Institutional Animal Care and Use Committee guidelines.

Murine B16F0 melanoma, L1.2 B lymphoma, and human 293 HEK lines were obtained from the American Type Culture Collection. Cell lines were grown in complete media consisting of RPMI 1640 supplemented with 10% FBS, sodium pyruvate, penicillin/streptomycin, and β-mercaptoethanol. To produce CMKLR1-, CCRL2-, or GPR1-positive cell lines, murine B16F0, L1.2, or human 293 cells were transfected with the gene for full-length murine CMKLR1, CCRL2, or GPR1, respectively, using the pcDNA3 expression vector (Invitrogen), and used in flow cytometry and RNA expression experiments as the positive control cell lines.

Chemerin receptor expression in tumor lines. To evaluate tumor lines for the known chemerin receptors (CMKLR1, CCRL2, and GPR1), untransfected tumor cells were stained with BZ194 or BZ186 (anti-CMKLR1), BZ2E3 (anti-CCRL2), and BZ043 (anti-GPR1), or their isotype control (BZ194, BZ043, and BZ2E3 isotype: rIgG2a; BZ186: mIgG1). BZ186, BZ194, and BZ2E3 have been previously described (Zabel et al., 2008; Graham et al., 2009); BZ043 is a rat monoclonal antibody against mGPR1 made in-house. Relative RNA expression of CMKLR1, CCRL2, and GPR1 by tumor cells was determined using reverse transcription and real-time

quantitative PCR (RT-qPCR). RT-qPCR was performed using Perfecta SYBR Green Supermix Reaction Mixes (Quanta BioSciences, Inc.) with primers against murine CMKLR1, CCRL2, or GPR1 and murine HPRT1. Receptor gene expression was normalized to the housekeeping gene mHPRT1, and relative expression levels were displayed using the $2^{-\Delta\Delta CT}$ method. "No reverse transcriptase" controls were performed and had negligible expression levels. Primers used were the following: mCMKLR1 forward, 5′-CGGTCTTCCTGGTGGTGA-3′; mCMKLR1 reverse, 5′-TTCGGGAAGGCCATGTGC-3′; mCCRL2 forward, 5′-TTCCAACATCCTCCTCCTTG-3′; mCCRL2 reverse, 5′-GTGGTATTGTTGCGTGCATC-3′;mGPR1forward,5′-GGAGCTCAGCATTCATCACA-3′; mGPR1 reverse, 5′-GCTGAAACCAAGAGCCTGTC-3′; mHPRT1 forward, 5′-TGTTGTTGGATATGCCCTTG-3′; and mHPRT1 reverse, 5′-GAGTCCTGTTGATGTTGCCA-3′.

Tumor transfections. The full-length gene that encodes murine prochemerin, murine *RARRES2*, was inserted into the cloning vector pcDNA3.1 (Invitrogen) using the XbaI and NotI restriction enzyme digestion sites. Restriction digests confirmed correct insertion. Cell lines were grown in RPMI complete media in 24-well plates and transfected using Lipofectamine or Lipofectamine Plus (Invitrogen) according to the manufacturer's protocol. Empty vector pcDNA3.1 neo was used to produce control or mock-transfected cells. G418 sulfate (Invitrogen) at 500 μg/ml was used for selection. Transfected cell lines were used as unselected bulk or selected cloned lines, as indicated. Both clones and bulk-transfected tumor lines were screened for chemerin expression by plating tumor cells at equivalent densities (100,200 k/ml) and volumes in 24-well plates and culturing for 24 h with RPMI complete media. Tumor-conditioned media was harvested and filtered and assayed using an ELISA specific for murine chemerin (R&D Systems), according to the manufacturer's protocol. Transfected tumor lines were also stained with fluorescently labeled antibodies against murine CD44, MHC I, and CD1d (BD) along with isotype controls.

Tumor in vitro proliferation. To evaluate in vitro proliferation, cells were plated in 100 μl in 96-well plates at 100 k/ml and left to incubate for either 24 or 48 h. 20 μl CellTiter 96 (Promega) was then added, and the plates were incubated at 37°C for 1–3 h, per the manufacturer's protocol. Plates were then read at 490 nm on a plate reader to determine tumor cell proliferative rates. Some experiments were confirmed by manually assessed growth rates by counting viable cells mixed with trypan blue on a hemocytometer. In some experiments, the untransfected parental cell line was cultured with increasing concentrations (0–1,000 ng/ml) of recombinant murine active chemerin (R&D Systems), and proliferation measured as above.

Animal tumor experiments. To evaluate the effect of constitutively secreted chemerin on tumor growth, control or chemerin-expressing B16 melanoma tumor cells (0.5×10^6 [Fig. 3, H and I; and Fig. 4, B and C] or 1×10^6 [Fig. 2, E and F; and Fig. 3, F and G]) were inoculated subcutaneously into mice. Tumor growth was measured every 2–4 d by calipers, and size was expressed as the product of perpendicular length by width in square millimeters. Mice were euthanized when tumor size reached ∼400 mm^2 or when tumor sites ulcerated (Fig. 3, H and I) or at day 17 (Fig. 2, E and F; and Fig. 3, F and G) to evaluate for TILs by FACS. To evaluate the effect of exogenous chemerin on tumor growth, tumor lines were inoculated as indicated. Recombinant, active, carrier-free murine chemerin (R&D Systems) was reconstituted in sterile PBS. Endotoxin levels were <1.0 EU per 1 μg of the protein by the limulus amebocyte lysate method, as reported by the manufacturer. Purified murine serum albumin (Sigma-Aldrich) or PBS was used as control as indicated. 50–100 μl chemerin or control was injected both inside and around the periphery of the tumor mass. Tumors were injected once daily as indicated with either control or chemerin. Tumors were either treated from time of inoculation or after establishment at approximately day 5–10, when tumors were palpable. For experiments using established tumors, mice were inoculated and randomly divided into two groups before treatment. For depletion experiments, wild-type mice were treated with anti–Asialo GM1 polyclonal antiserum (Wako Chemicals USA) to deplete NK cells. Anti–Asialo GM1 was reconstituted in water per the manufacturer's recommendations, diluted 1:10 in PBS, and 200 μl was injected i.p. the day before tumor inoculation. 100 μl was then injected i.p. on day 0, and every 3–4 d thereafter for the duration of the experiment. Sterile PBS was injected i.p. in an identical fashion in control groups. To ensure NK depletion, 50–100 ml of peripheral blood from mice undergoing NK cell depletion with anti–Asialo GM1 was collected by retroorbital bleed under isoflurane anesthesia at days 3–5 after first injection with anti–Asialo GM1. Red blood cell lysis was performed using ACK lysis buffer (Sigma-Aldrich). Samples were then stained for flow cytometry using anti-CD3 and either anti-NK1.1 or anti-DX5 monoclonal antibodies (as described in the next section). B6.129S7-*Rag1*^{tm1Mom}/J (RAG1 KO) mice were used in parallel with NK-depleted mice.

Flow cytometry analysis of ex vivo tumors. Whole subcutaneous tumors were resected en bloc, including the overlying and immediate surrounding skin and subcutaneous tissue. Tumors were then minced and mechanically disaggregated and passed through a 40-μM filter using ice-cold RPMI supplemented with 2% FBS to achieve a single cell suspension. Live cells were counted using trypan blue, and then samples were blocked with PBS/FBS containing 1% rat serum and Fc block (anti-CD16/32; BD). Samples were then stained with directly conjugated fluorescent antibodies against numerous murine leukocyte antigens and analyzed on an LSRII (BD). For live/dead cell discrimination, either propidium iodide or the AmCyan LIVE/DEAD Fixable Dead Cell Stain kit (Invitrogen) was used. The following antibodies were used (eBioscience): anti-CD3, CD4, CD8, CD11b, CD11c, CD19, CD45, B220, PDCA-1, NK1.1 or DX5, and GR1. FlowJo software (Tree Star) was used for analysis, and gatings were based on appropriate isotype control staining.

Immunofluorescence. For direct visualization of leukocyte infiltrates, control or chemerin-expressing tumors ($0.5–1 \times 10^6$ cells) were inoculated subcutaneously in wild-type mice. After 7–9 d, mice were euthanized, and tumors were resected and frozen in OCT freezing medium (Sakura). 10-μM sections were cut using a cryostat and then fixed in ice-cold acetone for 10 min. After air drying for 1 h, sections were blocked with PBS/BCS + 1% mouse serum for 30 min. Slides were then washed and stained with directly conjugated fluorescent murine antibodies (anti-CD45.2 FITC or isotype control murine IgG2a FITC; BD) diluted 1:1,000 in PBS/BCS for 30 min. Slides were washed and then stained with a 1:2,500 dilution of the nuclear dye Hoechst (Invitrogen) for 15 s. Slides were washed again, left to air dry, and mounted with coverslips. Sections were visualized using a fluorescent microscope (Eclipse TE300; Nikon).

Statistical analysis. Prism software (GraphPad Software) was used to plot tumor size and growth, tumor cell proliferation, chemerin and CMKLR1 expression, chemotaxis, and FACS results. InStat (GraphPad Software) was used to analyze differences between groups by applying an unpaired Student's *t* test or nonparametric Mann-Whitney test, as indicated. P-values of <0.05 were considered significant. Statistics used for human tumor outcome analyses are described in Analysis of the prognostic value of *RARRES2* expression in human malignancies.

This work is dedicated to the memory of Alvin L. Pachynski, Jr.

We would like to thank J. Pan for his critical review of the manuscript.

This work was supported by grants AI047822, AI072618, DK084647, and RC1-AI087257 from the National Institutes of Health (NIH) and a Merit Award from the Department of Veterans Affairs (to E.C. Butcher). R.K. Pachynski was supported by NIH T32 CA009287-30A1, an American Society of Clinical Oncology Young Investigator Award, and a California Breast Cancer Research Project Fellowship; B.A. Zabel was supported by NIH grant AI079320. H.A. Hadeiba is funded by the California Institute of Regenerative Medicine, was a recipient of an Investigator Career Award from the Arthritis Foundation, and was a fellow under NIH Training Grant AI07290. A.A. Alizadeh is supported by the Doris Duke Charitable Foundation

and the Leukemia and Lymphoma Society. J. Monnier was supported by fellowships from NIH T-32 training grants T32-AI0729025 and T32-AI07290-24 and American Cancer Society postdoctoral fellowship PF-12-052-01-CSM. H.E. Kohrt was supported by funding from the American Society of Hematology, Leukemia and Lymphoma Society, and Department of Defense. A.J. Gentles was supported by National Cancer Institute grant 5U54CA149145.

The authors declare no competing financial interests.

Author contributions: R.K. Pachynski, B.A. Zabel, and E.C. Butcher planned and designed experiments. R.K. Pachynski, H.A. Hadeiba, H.E. Kohrt, N.M. Tejeda, G.V. Sperinde, A.K. Holzer, C.D. Swanson, A. Edalati, and J. Monnier performed experiments. A.A. Alizadeh and A.J. Gentles contributed compiled human clinical data and provided analyses. R.K. Pachynski, B.A. Zabel, and E.C. Butcher reviewed data and wrote the paper.

Submitted: 6 October 2011
Accepted: 7 June 2012

REFERENCES

Apte, R.N., S. Dotan, M. Elkabets, M.R. White, E. Reich, Y. Carmi, X. Song, T. Dvozkin, Y. Krelin, and E. Voronov. 2006. The involvement of IL-1 in tumorigenesis, tumor invasiveness, metastasis and tumor-host interactions. *Cancer Metastasis Rev.* 25:387–408. http://dx.doi.org/10.1007/s10555-006-9004-4

Bierie, B., and H.L. Moses. 2010. Transforming growth factor beta (TGF-beta) and inflammation in cancer. *Cytokine Growth Factor Rev.* 21:49–59. http://dx.doi.org/10.1016/j.cytogfr.2009.11.008

Chakravarti, N., R. Lotan, A.H. Diwan, C.L. Warneke, M.M. Johnson, and V.G. Prieto. 2007. Decreased expression of retinoid receptors in melanoma: entailment in tumorigenesis and prognosis. *Clin. Cancer Res.* 13:4817–4824. http://dx.doi.org/10.1158/1078-0432.CCR-06-3026

Curran, M.A., W. Montalvo, H. Yagita, and J.P. Allison. 2010. PD-1 and CTLA-4 combination blockade expands infiltrating T cells and reduces regulatory T and myeloid cells within B16 melanoma tumors. *Proc. Natl. Acad. Sci. USA.* 107:4275–4280. http://dx.doi.org/10.1073/pnas.0915174107

Edgar, R., M. Domrachev, and A.E. Lash. 2002. Gene Expression Omnibus: NCBI gene expression and hybridization array data repository. *Nucleic Acids Res.* 30:207–210. http://dx.doi.org/10.1093/nar/30.1.207

Ernst, M.C., I.D. Haidl, L.A. Zúñiga, H.J. Dranse, J.L. Rourke, B.A. Zabel, E.C. Butcher, and C.J. Sinal. 2012. Disruption of the chemokine-like receptor-1 (CMKLR1) gene is associated with reduced adiposity and glucose intolerance. *Endocrinology.* 153:672–682. http://dx.doi.org/10.1210/en.2011-1490

Fernandez-Ranvier, G.G., J. Weng, R.F. Yeh, E. Khanafshar, I. Suh, C. Barker, Q.Y. Duh, O.H. Clark, and E. Kebebew. 2008. Identification of biomarkers of adrenocortical carcinoma using genomewide gene expression profiling. *Arch. Surg.* 143:841–846, discussion :846. http://dx.doi.org/10.1001/archsurg.143.9.841

Graham, K.L., B.A. Zabel, S. Loghavi, L.A. Zuniga, P.P. Ho, R.A. Sobel, and E.C. Butcher. 2009. Chemokine-like receptor-1 expression by central nervous system-infiltrating leukocytes and involvement in a model of autoimmune demyelinating disease. *J. Immunol.* 183:6717–6723. http://dx.doi.org/10.4049/jimmunol.0803435

Hadeiba, H., T. Sato, A. Habtezion, C. Oderup, J. Pan, and E.C. Butcher. 2008. CCR9 expression defines tolerogenic plasmacytoid dendritic cells able to suppress acute graft-versus-host disease. *Nat. Immunol.* 9:1253–1260. http://dx.doi.org/10.1038/ni.1658

Klopper, J.P., V. Sharma, A. Berenz, W.R. Hays, M. Loi, U. Pugazhenthi, S. Said, and B.R. Haugen. 2009. Retinoid and thiazolidinedione therapies in melanoma: an analysis of differential response based on nuclear hormone receptor expression. *Mol. Cancer.* 8:16. http://dx.doi.org/10.1186/1476-4598-8-16

Majeti, R., M.P. Chao, A.A. Alizadeh, W.W. Pang, S. Jaiswal, K.D. Gibbs Jr., N. van Rooijen, and I.L. Weissman. 2009. CD47 is an adverse prognostic factor and therapeutic antibody target on human acute myeloid leukemia stem cells. *Cell.* 138:286–299. http://dx.doi.org/10.1016/j.cell.2009.05.045

Maldonado, R.A., and U.H. von Andrian. 2010. How tolerogenic dendritic cells induce regulatory T cells. *Adv. Immunol.* 108:111–165. http://dx.doi.org/10.1016/B978-0-12-380995-7.00004-5

Muruganandan, S., S.D. Parlee, J.L. Rourke, M.C. Ernst, K.B. Goralski, and C.J. Sinal. 2011. Chemerin, a novel peroxisome proliferator-activated receptor gamma (PPARgamma) target gene that promotes mesenchymal stem cell adipogenesis. *J. Biol. Chem.* 286:23982–23995. http://dx.doi.org/10.1074/jbc.M111.220491

Nagaraj, S., and D.I. Gabrilovich. 2010. Myeloid-derived suppressor cells in human cancer. *Cancer J.* 16:348–353. http://dx.doi.org/10.1097/PPO.0b013e3181eb3358

Nagpal, S., S. Patel, H. Jacobe, D. DiSepio, C. Ghosn, M. Malhotra, M. Teng, M. Duvic, and R.A. Chandraratna. 1997. Tazarotene-induced gene 2 (TIG2), a novel retinoid-responsive gene in skin. *J. Invest. Dermatol.* 109:91–95. http://dx.doi.org/10.1111/1523-1747.ep12276660

Ostrand-Rosenberg, S. 2010. Myeloid-derived suppressor cells: more mechanisms for inhibiting antitumor immunity. *Cancer Immunol. Immunother.* 59:1593–1600. http://dx.doi.org/10.1007/s00262-010-0855-8

Parolini, S., A. Santoro, E. Marcenaro, W. Luini, L. Massardi, F. Facchetti, D. Communi, M. Parmentier, A. Majorana, M. Sironi, et al. 2007. The role of chemerin in the colocalization of NK and dendritic cell subsets into inflamed tissues. *Blood.* 109:3625–3632. http://dx.doi.org/10.1182/blood-2006-08-038844

Pivarcsi, A., A. Müller, A. Hippe, J. Rieker, A. van Lierop, M. Steinhoff, S. Seeliger, R. Kubitza, U. Pippirs, S. Meller, et al. 2007. Tumor immune escape by the loss of homeostatic chemokine expression. *Proc. Natl. Acad. Sci. USA.* 104:19055–19060. http://dx.doi.org/10.1073/pnas.0705673104

Sato, E., S.H. Olson, J. Ahn, B. Bundy, H. Nishikawa, F. Qian, A.A. Jungbluth, D. Frosina, S. Gnjatic, C. Ambrosone, et al. 2005. Intraepithelial CD8+ tumor-infiltrating lymphocytes and a high CD8+/regulatory T cell ratio are associated with favorable prognosis in ovarian cancer. *Proc. Natl. Acad. Sci. USA.* 102:18538–18543. http://dx.doi.org/10.1073/pnas.0509182102

Schreiber, R.D., L.J. Old, and M.J. Smyth. 2011. Cancer immunoediting: integrating immunity's roles in cancer suppression and promotion. *Science.* 331:1565–1570. http://dx.doi.org/10.1126/science.1203486

Segditsas, S., O. Sieber, M. Deheragoda, P. East, A. Rowan, R. Jeffery, E. Nye, S. Clark, B. Spencer-Dene, G. Stamp, et al. 2008. Putative direct and indirect Wnt targets identified through consistent gene expression changes in APC-mutant intestinal adenomas from humans and mice. *Hum. Mol. Genet.* 17:3864–3875. http://dx.doi.org/10.1093/hmg/ddn286

Sethi, G., B. Sung, and B.B. Aggarwal. 2008. TNF: a master switch for inflammation to cancer. *Front. Biosci.* 13:5094–5107. http://dx.doi.org/10.2741/3066

Shistik, G., A.V. Prakash, N.A. Fenske, and L.F. Glass. 2007. Treatment of locally metastatic melanoma: a novel approach. *J. Drugs Dermatol.* 6:830–832.

Skrzeczyńska-Moncznik, J., A. Stefanska, B.A. Zabel, M. Kapińska-Mrowiecka, E.C. Butcher, and J. Cichy. 2009. Chemerin and the recruitment of NK cells to diseased skin. *Acta Biochim. Pol.* 56:355–360.

Stamey, T.A., J.A. Warrington, M.C. Caldwell, Z. Chen, Z. Fan, M. Mahadevappa, J.E. McNeal, R. Nolley, and Z. Zhang. 2001. Molecular genetic profiling of Gleason grade 4/5 prostate cancers compared to benign prostatic hyperplasia. *J. Urol.* 166:2171–2177. http://dx.doi.org/10.1016/S0022-5347(05)65528-0

Su, A.I., T. Wiltshire, S. Batalov, H. Lapp, K.A. Ching, D. Block, J. Zhang, R. Soden, M. Hayakawa, G. Kreiman, et al. 2004. A gene atlas of the mouse and human protein-encoding transcriptomes. *Proc. Natl. Acad. Sci. USA.* 101:6062–6067. http://dx.doi.org/10.1073/pnas.0400782101

Winnepenninckx, V., V. Lazar, S. Michiels, P. Dessen, M. Stas, S.R. Alonso, M.F. Avril, P.L. Ortiz Romero, T. Robert, O. Balacescu, et al; Melanoma Group of the European Organization for Research and Treatment of Cancer. 2006. Gene expression profiling of primary cutaneous melanoma and clinical outcome. *J. Natl. Cancer Inst.* 98:472–482. http://dx.doi.org/10.1093/jnci/djj103

Wittamer, V., J.D. Franssen, M. Vulcano, J.F. Mirjolet, E. Le Poul, I. Migeotte, S. Brézillon, R. Tyldesley, C. Blanpain, M. Detheux, et al. 2003. Specific recruitment of antigen-presenting cells by chemerin, a

novel processed ligand from human inflammatory fluids. *J. Exp. Med.* 198:977–985. http://dx.doi.org/10.1084/jem.20030382

Xu, L., S.S. Shen, Y. Hoshida, A. Subramanian, K. Ross, J.P. Brunet, S.N. Wagner, S. Ramaswamy, J.P. Mesirov, and R.O. Hynes. 2008. Gene expression changes in an animal melanoma model correlate with aggressiveness of human melanoma metastases. *Mol. Cancer Res.* 6:760–769. http://dx.doi.org/10.1158/1541-7786.MCR-07-0344

Zabel, B.A., A.M. Silverio, and E.C. Butcher. 2005. Chemokine-like receptor 1 expression and chemerin-directed chemotaxis distinguish plasmacytoid from myeloid dendritic cells in human blood. *J. Immunol.* 174:244–251.

Zabel, B.A., L. Zuniga, T. Ohyama, S.J. Allen, J. Cichy, T.M. Handel, and E.C. Butcher. 2006. Chemoattractants, extracellular proteases, and the integrated host defense response. *Exp. Hematol.* 34:1021–1032. http://dx.doi.org/10.1016/j.exphem.2006.05.003

Zabel, B.A., S. Nakae, L. Zúñiga, J.Y. Kim, T. Ohyama, C. Alt, J. Pan, H. Suto, D. Soler, S.J. Allen, et al. 2008. Mast cell-expressed orphan receptor CCRL2 binds chemerin and is required for optimal induction of IgE-mediated passive cutaneous anaphylaxis. *J. Exp. Med.* 205:2207–2220. http://dx.doi.org/10.1084/jem.20080300

Zheng, Y., S. Luo, G. Wang, Z. Peng, W. Zeng, S. Tan, Y. Xi, and J. Fan. 2008. Downregulation of tazarotene induced gene-2 (TIG2) in skin squamous cell carcinoma. *Eur. J. Dermatol.* 18:638–641.

Zitvogel, L., A. Tesniere, and G. Kroemer. 2006. Cancer despite immunosurveillance: immunoselection and immunosubversion. *Nat. Rev. Immunol.* 6:715–727. http://dx.doi.org/10.1038/nri1936